ZEUS-prel-05-022-plus

Submitted to the
XXXIII International Conference on High Energy Physics
26 July - 2 August 2006, Moscow, Russia

Sessions: QCD hard interactions/QCD soft interactions/Heavy quark physics

Diffractive photoproduction of $D^{*\pm}(2010)$ mesons at HERA

ZEUS Collaboration

Abstract

Diffractive photoproduction of $D^{*\pm}$ mesons has been measured with the ZEUS detector at HERA using an integrated luminosity of 78.6 pb^{-1}. D^* mesons have been reconstructed with the transverse momentum $P_T(D^*) > 1.9\,\text{GeV}$ and pseudorapidity $|\eta(D^*)| < 1.6$ from the decay channel $D^{*+} \to D^0\pi^+$ with $D^0 \to K^-\pi^+$ (+c.c.). Diffractive events were identified by a large gap in the rapidity distribution of final state particles. The cross section integrated over the kinematic range as well as differential cross sections have been measured for photon-proton centre-of-mass energies $130 < W < 300$ GeV, photon virtualities $Q^2 < 1\,\text{GeV}^2$ and Pomeron fractional momentum $0.001 < x_{I\!P} < 0.035$. The results are compared to theoretical expectations.

1 Introduction

Charm-production processes proceed mainly through gluon–initiated hard subprocesses and are calculable in perturbative QCD (pQCD). Thus, the diffractive production of charmed mesons can provide information on the partonic structure of diffractive interactions, in particular of their gluon component.

Inclusive charm production at HERA has been measured [1, 2] in photoproduction reactions with photon virtualities, Q^2, close to zero, and in deep inelastic scattering (DIS) for $Q^2 \gtrsim 1$ GeV^2. The measured cross sections for photoproduction and deep inelastic scattering processes were compared with next-to-leading (NLO) QCD calculations. The calculations were found to be in good agreement with the DIS data. The calculated photoproduction cross sections are lower than the measurements, especially in the forward (proton) direction. Measured cross sections of diffractive D^* production in DIS at HERA [3, 4] have shown reasonable agreement with predictions of the two-gluon exchange models and the resolved Pomeron ($I\!P$) model assuming that diffractive exchange is dominated by gluons.

In this paper, results on diffractive photoproduction of $D^{*\pm}(2010)$[1] mesons are presented for the Pomeron fractional momentum $0.001 < x_{I\!P} < 0.035$. The measurement was performed in a wider kinematic range and with much larger statistics than previously [5]. The photon–proton centre-of-mass energy was $130 < W < 300\,\text{GeV}$, and photon virtualities were $Q^2 < 1\,\text{GeV}^2$. D^* mesons were reconstructed through the decay channel $D^{*+} \to D^0\pi_s^+ \to (K^-\pi^+)\pi_s^+$ (and c.c.) in the restricted kinematic region $P_T^{D^*} > 1.9\,\text{GeV}$ and $|\eta^{D^*}| < 1.6$. Here $P_T^{D^*}$ is the D^* transverse[2] momentum and $\eta^{D^*} = -\ln(\tan\frac{\theta}{2})$ is its pseudorapidity, defined in terms of the D^* polar angle θ with respect to the proton beam direction.

The measurement was performed at the HERA collider with the ZEUS detector, a detailed description of which can be found elsewhere [6]. The data were taken during 1998 - 2000, when HERA collided lepton (positron or electron)[3] and proton beams with energies of 27.5 GeV and 920 GeV, respectively. A summed integrated luminosity of $78.6\,\text{pb}^{-1}$ ($13.5\,\text{pb}^{-1}$ and $65.1\,\text{pb}^{-1}$ for e^-p and e^+p, respectively) was used for this measurement. Charged particles were measured in the central tracking detector (CTD) [7]. To check for the absence of the scattered electron and to measure global energy values, the uranium-scintillator sampling calorimeter (CAL) [8] was used. The online selection was performed

[1] In the following, $D^{*\pm}(2010)$ will be referred to simply as D^*.

[2] The ZEUS coordinate system is a right-handed Cartesian system, with the Z axis pointing in the proton beam direction, referred to as the "forward direction", and the X axis pointing left towards the center of HERA. The coordinate origin is at the nominal interaction point.

[3] Hereafter, both e^+ and e^- are referred to as electrons, unless explicitly stated otherwise.

with a three-level trigger system [9]. The forward plug calorimeter (FPC) [10] was used to suppress the non-diffractive backgrounds and reject the proton dissociation contribution. The luminosity was determined from the rate of the bremsstrahlung process $e^+p \to e^+\gamma p$, where the photon was measured by a lead scintillator calorimeter [11].

2 Kinematics of diffractive photoproduction

Diffractive photoproduction in ep scattering at HERA,

$$e + p \to e' + X + p',$$

can be described in terms of the four-momenta of the incoming and outgoing electron, e and e', and of the incoming and outgoing proton, p and p'. The kinematic variables include the squared electron–proton centre-of-mass energy, $s = (e+p)^2$, the photon virtuality, $Q^2 = -q^2$, where $q = e - e'$, and the squared photon–proton centre-of-mass energy, $W^2 = (p+q)^2$. The process can be considered to proceed through virtual photon–Pomeron ($I\!P$) interaction:

$$\gamma^*(q) + I\!P(P_{I\!P}) \to X,$$

where $P_{I\!P} = p - p'$. This process is described by the invariant mass, M_X, of the hadronic system X, produced by photon dissociation, and the fraction of the proton momentum

$$x_{I\!P} = \frac{P_{I\!P} \cdot q}{p \cdot q} \simeq \frac{M_X^2}{W^2}$$

carried away by the Pomeron.

The variables W, M_X and $x_{I\!P}$ were reconstructed from the hadronic final state, using a combination of track and calorimeter information that optimises the resolution of reconstructed kinematic variables [12]. The selected tracks and calorimeter clusters are referred to as Energy Flow Objects (EFOs). The Jacquet–Blondel formula [13]

$$W_{\rm JB} = \sqrt{2E_p \sum_i (E - P_z)_i}$$

was used to reconstruct W, where E_p is the proton beam energy. The invariant mass of the diffractively produced system, M_X, was calculated with the formula

$$M_X^2 = \left(\sum_i E_i\right)^2 - \left(\sum_i P_{x_i}\right)^2 - \left(\sum_i P_{y_i}\right)^2 - \left(\sum_i P_{z_i}\right)^2.$$

The sums in both equations run over energies E_i and momenta P_i of all clusters. [1]. The measured values were corrected for energy losses in inactive material of the ZEUS detector and for the loss of particles down the beam pipe which remained undetected. They were corrected by means of a parametrisation, obtained with the Monte Carlo (MC) simulations of diffraction. All variables were reconstructed with resolutions better than 15%.

3 Event simulation

The diffractive process $ep \to eXp \to e(D^{*\pm}X')p$ was modelled with the RAPGAP [16] program in the framework of the resolved Pomeron model [17] with the H1FIT2 LO [18] parameterization for the initial partonic distributions of the Pomeron and a small admixture of Reggeon exchange. In this measurement the final-state proton was not detected. To estimate and subtract the contribution from the proton dissociative processes $ep \to eXN \to e(D^{*\pm}X')N$, where the proton dissociates into a system N, the DIFFVM [19] program was used. The PYTHIA [20] and the HERWIG [21] programs were used to model non-diffractive interactions. The CTEQ5L [22] and GRV LO [23] parameterizations were used in both models for the proton and photon parton density functions, respectively. The fragmentation of the generated partons (parton shower evolution and hadronization) was simulated according to the LUND model [24] when using the RAPGAP or the PYTHIA simulations. In the HERWIG generator hadronization is described with a cluster hadronization model [25]. The charm mass was set to $m_c = 1.5$ GeV. The MC events were passed through the standard ZEUS detector and trigger simulation programs (based on the GEANT program [26]) and through the same event reconstruction package as was used for the data processing. The shapes of the MC and data distributions were found to be in reasonable agreement.

4 Event selection and D^* reconstruction

Event selection and D^* reconstruction procedures are described in detail elsewhere [1]. Photoproduction events were selected by requiring that no scattered electron was identified in the CAL [14] and that $130 < W < 300$ GeV. Under these conditions, Q^2 is limited to values below 1 GeV^2. The corresponding median Q^2 was estimated from a MC simulation to be about 3×10^{-4} GeV^2. The D^* mesons were reconstructed in the decay channel $D^{*+} \to (D^0 \to K^-\pi^+)\pi_s^+(+c.c.)$. For the reconstruction, "right charge" track combinations, defined for the $(K\pi)$ as two tracks of opposite charges and with a π_s having the charge opposite to that of the K meson, were accepted as long as the combination of invariant masses $\Delta M = M(K\pi\pi_s) - M(K\pi)$ and $M(K\pi)$ were within wide mass-windows around the nominal values of $\Delta M = M(D^*) - M(D^0)$ and $M(D^0)$ [15]. For selected D^* candidates, consistency of the $M(K\pi)$ value with the nominal D^0 mass was required. To account for the $M(K\pi)$ resolution, the requirement was varied from $1.82 < M(K\pi) < 1.91$ GeV for the lower $P_T^{D^*}$ up to $1.79 < M(K\pi) < 1.94$ GeV for the higher $P_T^{D^*}$. Cuts on transverse momentum of the D^*, $P_T^{D^*} > 1.9$ GeV and a ratio of $P_T^{D^*}/E_T^{\theta>10^o} > 0.1$, were applied to suppress combinatorial background. Here $E_T^{\theta>10^o}$ is the transverse energy, measured in the CAL outside a cone of $\theta = 10^o$ in the forward direction The combinatorial background was modelled by "wrong charge" track combinations and subtracted after normalization to the right charge distribution in the range $0.15 < \Delta M < 0.17$ GeV. The wrong charge combinations were defined for $(K\pi)$ as two tracks of the same charges and with a π_s of the opposite charge. The measurements were performed in the pseudorapidity range $-1.6 < \eta^{D^*} < 1.6$, where the CTD acceptance is high.

Diffractive events were identified by a large rapidity gap (LRG) between the scattered proton, which escaped undetected through the beam pipe, and the hadronic system X, produced by the dissociated photon. The LRG events were identified using the $\eta_{\rm max}$ method [27], where $\eta_{\rm max}$ is the pseudorapidity of the most forward EFO with energy greater than 400 MeV. Fig. 1a shows the $\eta_{\rm max}$ distribution for all photoproduced D^* mesons reconstructed within the signal range $0.1435 < M(K\pi\pi_s) - M(K\pi) < 0.1475$ GeV after the combinatorial background subtraction. This distribution shows two structures. The plateau-like structure at the lower $\eta_{\rm max}$ values ($\eta_{\rm max} \lesssim 2$) is dominated by the diffractive events, while the wide peak-like structure around $\eta_{\rm max} \sim 3.5$ originates from the non-diffractive events and has an exponential fall-off towards lower values of η_{max}. The non-diffractive contribution was strongly suppressed by the requirement $E_{\rm FPC} < 1.5$ GeV (Fig. 1b), where $E_{\rm FPC}$ is the energy deposited in the FPC. Restricting the selection to $\eta_{\rm max} < 3$ in addition reduces the remaining non-diffractive background and ensures a gap of at least two units of pseudorapidity with respect to the edge of the forward calorimetric coverage enlarged by the FPC up to $\eta \sim 5$. The $\eta_{\rm max}$ distribution, obtained for the selected data sample, was fitted with a sum of diffractive and non-diffractive MC simulations and an estimate for the non-diffractive admixture of 3.6% was obtained from PYTHIA. The difference between the HERWIG and PYTHIA predictions was used as a systematic uncertainty for this contribution. After the above selections and the wrong charge background subtraction, a signal of 454 ± 30 diffractively photoproduced D^* mesons was found (Fig. 2).

The measured range of rapidities is limited by the edge of the hole through which the beam-pipe passes in the forward direction. Thus, proton-dissociative events, $ep \rightarrow e'XN$, can satisfy the requirement $\eta_{\rm max} < 3$ in case the major part of the proton-dissociative hadronic system, N, passes undetected through the forward beam-pipe. Using the method, developed previously [4], the proton-dissociative contribution was determined to be 16% with negligible statistical uncertainty and a systematic uncertainty of $\pm$ 4%. Measured cross sections were corrected for this value. A cut in $\eta_{\max}$ correlates with a range of accessible $x_{I\!P}$ values. In particular, $\eta_{\max} < 3$ restricts the measurement to $x_{I\!P} < 0.035$. In addition, limited acceptance restricts $x_{I\!P} > 0.001$.

5 Cross sections

The cross section of D^* production is given by:

$$\sigma_{ep\to D^*X} = \frac{N^{\rm corr}_{D^*}}{\mathcal{L}\cdot B_{D^*\to(D^0\to K\pi)\pi}} \ ,$$

where $N^{\rm corr}_{D^*}$ is the number of observed D^* mesons corrected for backgrounds (non-diffractive and proton-dissociative) and the acceptance, $\mathcal{L} = 78.6 \pm 1.7\,{\rm pb}^{-1}$ is the integrated luminosity and $B_{D^*\to(D^0\to K\pi)\pi} = 0.0257{\pm}0.0006$ is the combined $D^* \to (D^0 \to K^+\pi^-)\,\pi_s$ decay branching ratio [15].

The cross section of diffractive photoproduction of D^* mesons integrated over the kinematic region $Q^2 < 1$ GeV^2, $130 < W < 300$ GeV, $P_T^{D^*} > 1.9$ GeV, $|\eta^{D^*}| < 1.6$ and $0.001 < x_{I\!P} < 0.035$ is

$$\sigma^{\rm diff}_{ep\to e'D^*X'p} = 1.57 \pm 0.12({\rm stat.})^{+0.20}_{-0.22}({\rm syst.}) \pm 0.08({\rm p.diss.})\ \ {\rm nb}.$$

The last uncertainty is due to the uncertainty in the proton dissociation subtraction. Other sources of systematic uncertainties due to analysis and detector features were studied and their effect on the cross section was evaluated. The largest contributions to the systematic uncertainty comes from the signal determination procedure, the selection of diffractive events and the acceptance correction calculations. All of the systematic uncertainties were added in quadrature to determine the overall systematic uncertainty. The overall normalization uncertainties due to the uncertainties in the luminosity ($\pm 2.2\%$), in the D^* and D^0 decay branching ratios ($\pm 2.5\%$) and proton-dissociation subtraction ($\pm 4.8\%$, given separately) were not included in the systematic uncertainty calculation.

The measured diffractive photoproduction cross section of D^* is sizeable in comparison to $18.9 \pm 1.2^{+1.8}_{-0.8}$ nb of the inclusive D^* photoproduction cross section, measured in a similar kinematic range [1]. This observation indicates that diffractive charm production is not suppressed as much as some early models predicted [29].

The measurements are compared to the LO expectations from the resolved-Pomeron model [17] calculated in the same kinematic region. Both boson-gluon fusion and resolved photon mechanisms of charm production were simulated by the RAPGAP MC program, with the resolved component amounting for $\sim 35\%$ of their sum. The LO calculations, based on the H1FIT2 LO Pomeron parton density parameterization, determined from the HERA DIS data, predict 4.27 nb for the diffractive photoproduction cross section of the

D^* in the above kinematic range [30], overestimating the current measurement by factor of 2.7.

Differential cross sections for $d\sigma/dP_T^{D^*}$, $d\sigma/d\eta^{D^*}$, $d\sigma/dM_X$, $d\sigma/dx_{I\!P}$ and $d\sigma/dW$ are presented in Figs. 3-7. calculated with the RAPGAP MC program from the resolved-Pomeron model, show reasonable agreement in shape with the measurements. The calculation is multiplied by a factor of 0.37 to get the right normalization to the measured cross section. Scaling the resolved component by 0.34 [31] would not give a substantially better description of the data in both shape and normalisation. However, the normalisation in the RAPGAP MC suffers from significant uncertainties. More definite conclusions will be possible with a NLO prediction of this process.

6 Summary and conclusions

Diffractive photoproduction of D^* mesons has been measured with the ZEUS detector at HERA using an integrated luminosity of $78.6\,\mathrm{pb}^{-1}$. D^* mesons were reconstructed with $P_T^{D^*} > 1.9\,\mathrm{GeV}$, $|\eta^{D^*}| < 1.6$. The cross section for diffractive photoproduction of D^* integrated over the kinematic region $Q^2 < 1\mathrm{GeV}^2$, $130 < W < 300\,\mathrm{GeV}$ and $0.001 < x_{I\!P} < 0.035$ is measured to be

$$\sigma^{\mathrm{diff}}_{ep\to e'D^*Xp'} = 1.57 \pm 0.12(\mathrm{stat.})^{+0.20}_{-0.22}(\mathrm{syst.}) \pm 0.08(\mathrm{p.diss.})\,\mathrm{nb}.$$

A leading-order calculation in the framework of the resolved-Pomeron model, based on gluon dominated parton densities H1FIT2, predict 4.27 nb for this cross section. The shapes of the differential cross sections for the resolved-Pomeron model show reasonable agreement with the measurements of $d\sigma/dP_T^{D^*}$, $d\sigma/d\eta^{D^*}$, $d\sigma/dM_X$, $d\sigma/dx_{I\!P}$ and $d\sigma/dW$.

7 Acknowledgments

We would like to thank the DESY Directorate for their strong support and encouragement. The remarkable achievements of the HERA machine group were essential for this work and are greatly appreciated. We would like to thank H. Jung for fruitful discussions and help in the use of the RAPGAP MC generator.

References

[1] ZEUS Coll., M. Derrick et al., Phys. Lett. **B 349**, 225 (1995);
ZEUS Coll., J. Breitweg et al., Phys. Lett. **B 401**, 192 (1997);
ZEUS Coll., J. Breitweg et al., Phys. Lett. **B 407**, 402 (1997);
ZEUS Coll., J. Breitweg et al., Eur. Phys. J. **C 6**, 67 (1999);
ZEUS Coll., J. Breitweg et al., Eur. Phys. J. **C 12**, 35 (2000);
ZEUS Coll., Paper 786, 31th Int. Conf. on High Energy Phys. ICHEP02, Amsterdam, The Netherlands, 2002;
ZEUS Coll., S. Chekanov et al., Phys. Rev. **D 69**, 0120004(2004).

[2] H1 Coll., S. Aid et al., Nucl. Phys. **B 472**, 32 (1996);
H1 Coll., C. Adlof et al., Z. Phys. **C 72**, 593 (1996);
H1 Coll., C. Adloff et al., Phys. Lett. **B 528**, 199 (2002);
H1 Coll., C. Adloff et al., Nucl. Phys. **B 545**, 21 (1999).

[3] H1 Coll., C. Adloff et al., Phys. Lett. **B 520**, 191 (2001)
H1 Coll., A. Aktas et al., Eur. Phys. J. **C 38**, 447 (2005).

[4] ZEUS Coll., S. Chekanov et al., Phys. Lett. **B 545**, 244 (2002);
ZEUS Coll., S. Chekanov et al., Nucl. Phys. **B 672**, 3 (2003).

[5] ZEUS Coll., Paper 489, *Int. Europhys. Conf. on High Energy Phys., Budapest, Hungary, 2001.*

[6] ZEUS Coll., M. Derrick et al., Phys. Lett. **B 293**, 465 (1992);
ZEUS Coll., U. Holm (ed.), *The ZEUS detector.* Status Report DESY (unpublished), 1993, available on `http://www-zeus.desy.de/bluebook/bluebook.html`.

[7] N. Harnew et al., Nucl. Instr. Meth. **A 279**, 290 (1989);
B. Foster et al., Nucl. Phys. Proc. Suppl. **B 32**, 181 (1993);
B. Foster et al., Nucl. Instr. Meth. **A 338**, 254 (1994).

[8] M. Derrick et al., Nucl. Inst. Meth. **A 309**, 77 (1991);
A. Andresen et al., Nucl. Inst. Meth. **A 309**, 101 (1991);
A. Caldwell et al., Nucl. Inst. Meth. **A 321**, 356 (1992);
A. Bernstein et al., Nucl. Inst. Meth. **A 336**, 23 (1993).

[9] W. H. Smith, K. Tokushuku and L. W. Wiggers, Proc. Computing in High-Energy Physics (CHEP), Annecy, France, Sept. 1992;
C. Verkerk and W. Wojcik (eds.), p. 222. CERN, Geneva, Switzerland (1992), preprint DESY 92-150B.

[10] A. Bamberger et al., Nucl. Inst. Meth. **A 450**, 235 (2000).

[11] J. Andruszków et al., DESY 92-066, 1992;
ZEUS Coll., M.Derrick et al., Z. Phys. **C 63**, 391 (1994).

[12] ZEUS Coll., J. Breitweg et al., Eur. Phys. J. **C 1**, 81 (1998);
ZEUS Coll., J. Breitweg et al., Eur. Phys. J. **C 6**, 43 (1999);
G. Briskin, PhD Thesis, Tel Aviv University, Israel, 1998.

[13] F. Jacquet and A. Blondel, in *Proc. of the Study for an ep Facility for Europe*, U. Amaldi (ed.), p. 391, Hamburg, Germany (1979).

[14] ZEUS Coll., M. Derrick et al., Phys. Lett. **B 322**, 287 (1994).

[15] Particle Data Group, S. Eidelman et al., Phys. Lett. **B 592**, 1 (2004).

[16] H. Jung, Comp. Phys. Comm. **86**, 147 (1995).

[17] G. Ingelman and P. Schlein, Phys. Lett. **B 152**, 256 (1985);
A. Donnachie and P.V. Landshoff, Nucl. Phys. **B 303**, 634 (1988).

[18] H1 Coll., C. Adloff et al., Z. Phys. **C 76**, 613 (1997).

[19] B. List and A. Mastroberardino, Proc. Workshop on Monte Carlo Generators for HERA Physics, p. 396. DESY, Hamburg, Germany (1999), preprint DESY-PROC-1999-02, available on http://www.desy.de/ heramc/.

[20] T. Sjöstrand, Comp. Phys. Comm. **82**, 74 (1994).

[21] G. Marchesini et al., Comp. Phys. Comm. **67**, 465 (1992).

[22] H.L. Lai etal., Eur. Phys. J **C 12**, 375 (2000).

[23] M. Glück, E. Reya, and A. Vogt, Phys. Rev. **D 46**, 1973 (1992).

[24] T. Sjöstrand, Comp. Phys. Comm. **39**, 347 (1986);
T. Sjöstrand and M. Bengtsson, Comp. Phys. Comm. **43**, 367 (1987).

[25] B. R. Webber, Nucl. Phys. **B 238**, 492 (1984).

[26] R. Brun et al., GEANT3, Technical Report CERN-DD/EE/84-1, CERN, 1987.

[27] ZEUS Coll., M. Derrick et al., Phys. Lett. **B 315**, 481 (1993).

[28] ZEUS Coll., J. Breitweg et al., Eur. Phys. J. **C 6**, 43 (1999).

[29] N.N. Nikolaev and B.G. Zakharov, Z. Phys. **C 53**, 331 (1992).

[30] H. Jung, private communication, 2000.

[31] A.B. Kaidalov et al., Phys. Lett. **B 567**, 61 (2003)

Addendum: comparison to NLO calculations

The cross sections of diffractive photoproduction of D^* mesons were calculated in next-to leading order (NLO) QCD using the FMNR code [1]. Electroproduction with small photon virtualities was considered in the Weizsacker-Williams approximation [2]. The following diffractive parton density functions (dPDFs) are measured from NLO DGLAP QCD fits to the HERA inclusive data on diffraction in DIS: The H1 2006 Fits A and B [3], the ZEUS LPS Fit [4] and the GLP Fit [5]. The photon parton density AFG-G HO set [6] was used. The renormalization scale was taken as $\mu_R = \sqrt{p_{c,T}^2 + m_c^2}$, and the factorization scale for the photon and for the proton was taken as $\mu_F = \mu_R$. Here $p_{c,T}$ stands for the transverse momentum of the charm quark with mass $m_c = 1.45\,\text{GeV}$. Fragmentation of the final state quarks was described by the Peterson fragmentation function [7] with $\epsilon = 0.035$. The fragmentation fraction is set to 0.235. The calculations were performed with the value of $\alpha_s(M_Z^2) = 0.118$ in accord with the value used in all dPDF fits. Calculation uncertainties were estimated by simultaneous variations of the factorization and renormalisation scales by a factor $\mathcal{F}_\mu = 2.0(0.5)$ and of the charm quark mass by $\Delta m_c = +0.2(-0.2)\,\text{GeV}$.

Differential cross sections for $d\sigma/dP_T^{D^*}$, $d\sigma/d\eta^{D^*}$, $d\sigma/dM_X$, $d\sigma/dx_{I\!P}$ and $d\sigma/dW$ are presented in Figs. 8-12. The measurements are compared to the NLO QCD calculations, performed in the same kinematic region and shown as histograms in the same figures. The estimated calculation uncertainties, typically of the order 10-50 %, are shown as shaded bands for the results with dPDFs from H1 2006 Fit A. The uncertainties for the results with dPDFs from H1 2006 Fit B, ZEUS LPS Fit and GLP Fit are similar and not shown.

Apart from underestimating the diffractive charm photoproduction in the forward (proton) direction, the data are consistent with the NLO predictions based on H1's Fits A and B, as well as the ZEUS LPS Fit. The normalization of the prediction of the GLP Fit is substantially lower than those from the other fits. There are a number of possible explanations for the differences between the three sets of fits, including different fitting procedures and differences in the selection of the diffractive samples used for the fits. While not fully understood, the spread in the predictions may be taken as an estimate of their uncertainty at this point in time. This prevents, for the moment, a firm conclusion on the validity of hard diffractive factorisation.

References

[1] S. Frixione, M.L. Mangano, P. Nason and G. Ridolfi, Nucl. Phys. B412 225(1994)

[2] C.F. von Weizsacker, Z. Phys. 88, 612-625 (1934) E.J. Williams, Phys. Rev. 45, 729(1934)

[3] H1 Collab., A. Aktas et al., Submitted to Eur. Phys. J.C Submitted to Eur. Phys. J.C, DESY-06-049, hep-ex/0606004

[4] ZEUS Collaboration; S. Chekanov et al. European Physical Journal C 38 (2004) 43-67

[5] M. Groys, A. Levy and A. Proskuryakov, the Proc. of the HERALHC Workshop, DESY/CERN (2005).

[6] P. Aurenche, J. Guillet, M. Fontannaz, Z. Phys. C 64, 621(1994)

[7] C. Peterson, D. Schlatter, I. Schmitt and P. Zerwas, Phys. Rev. D27, 105(1983)

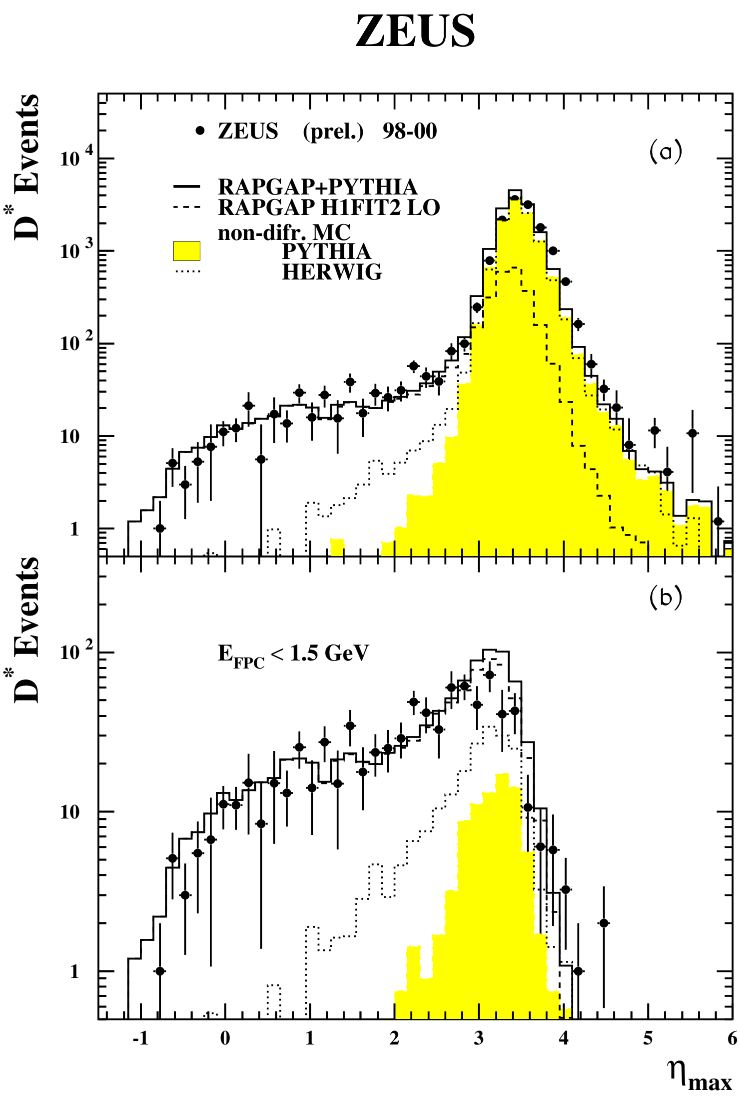

Figure 1: *Comparison of the measured $\eta_{\rm max}$ distribution (dots) with the sum of the diffractive and non-diffractive MC distributions (histograms) without a cut in E_{FPC} (a) and with $E_{FPC} < 1.5$ GeV (b) for events with reconstructed D^* mesons. The sum (solid histogram) of the diffractive resolved Pomeron RAPGAP MC (dashed histogram) and non-diffractive PYTHIA MC (filled histogram) events was normalised to have the same area as the data. The dotted histogram shows the non-diffractive HERWIG MC event distribution.*

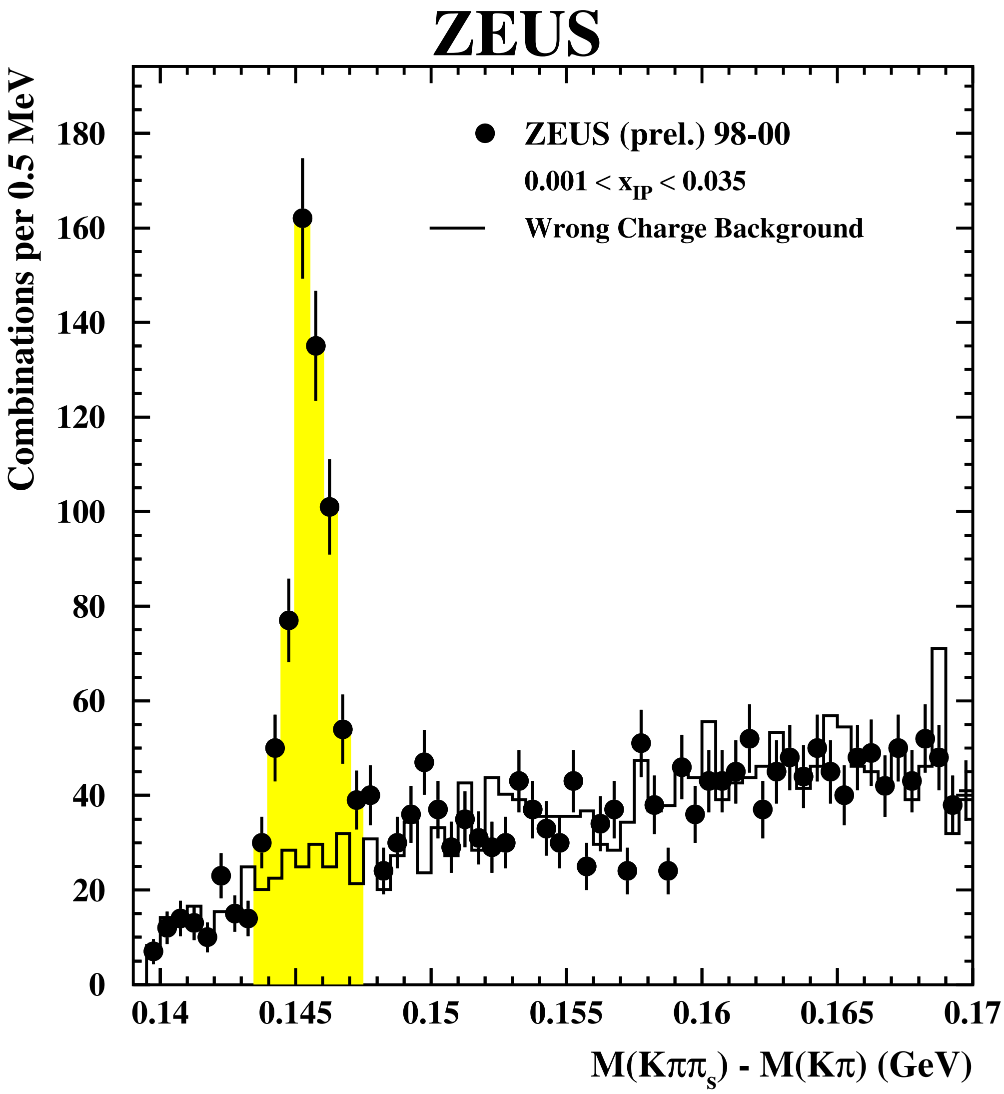

Figure 2: *The distribution of the mass difference* $\Delta M = M(K\pi\pi) - M(K\pi)$ *for* D^* *candidates(dots) from the diffractive reaction* $ep \rightarrow eD^*X'p$ *with* $0.001 < x_{I\!P} < 0.035$. *The histogram shows the combinatorial background, reproduced by wrong charge combinations. Only* D^* *candidates from the shaded area were used for the cross-section measurements*

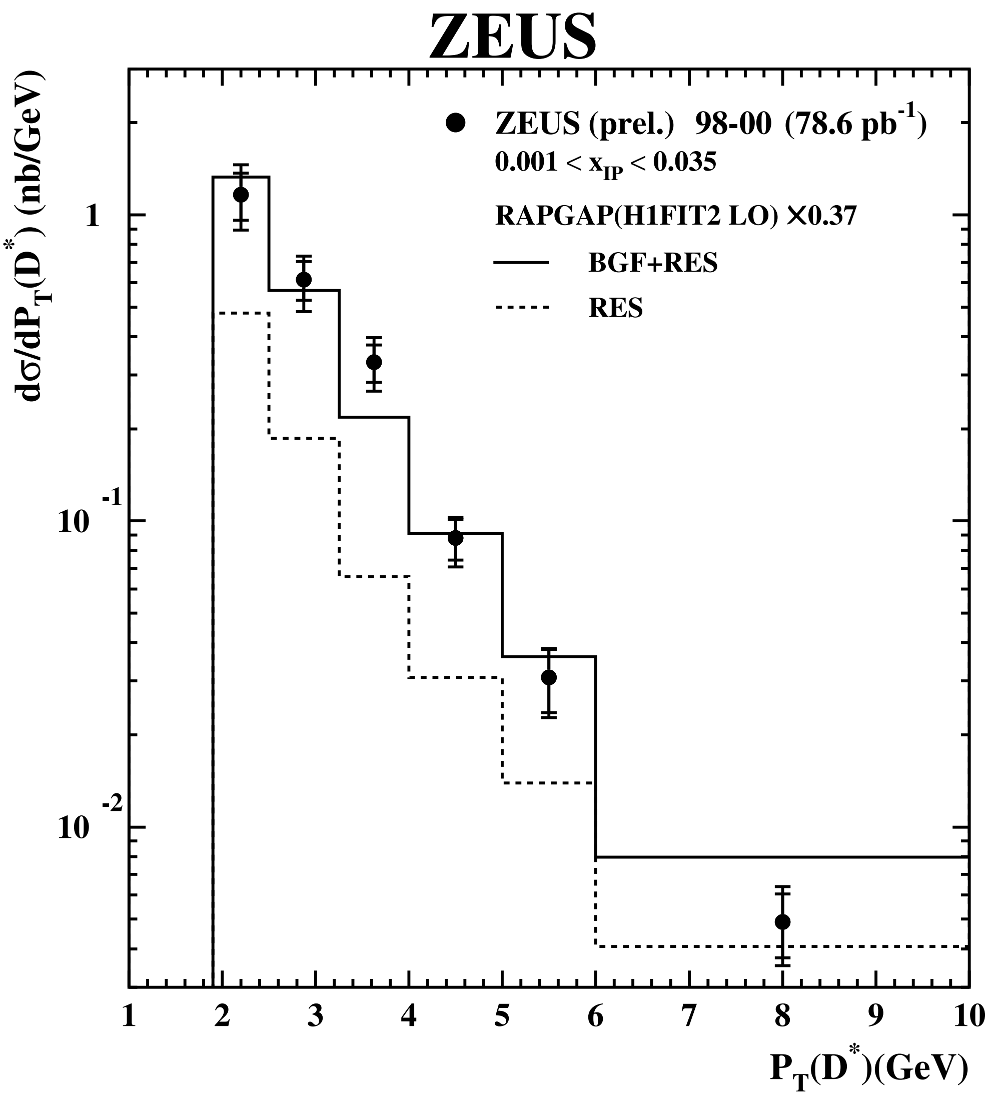

Figure 3: *The cross section $d\sigma/dP_T^{D^*}$ (dots) for the diffractive photoproduction reaction $ep \to eD^*X'p$ with $0.001 < x_{I\!P} < 0.035$. The inner bars show the statistical uncertainties, and the outer bars correspond to the statistical and systematic uncertainties, added in quadrature. The data are compared to the resolved Pomeron model predictions with the H1FIT2 LO Pomeron parametrization (histogram). The theoretical cross section was normalized to the data. The dashed histogram shows the predicted contribution from resolved photon reactions.*

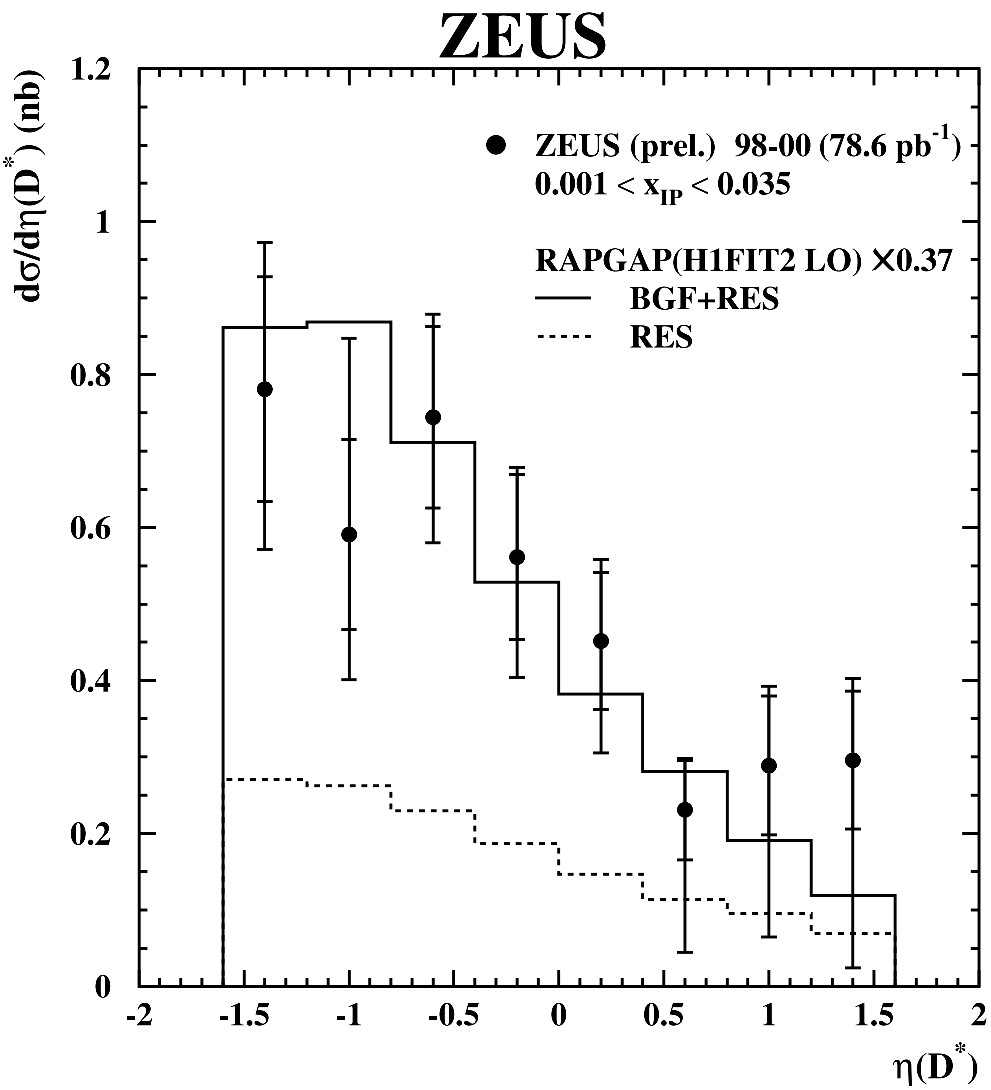

Figure 4: *The cross section* $d\sigma/d\eta^{D^*}$ *(dots) for the diffractive photoproduction reaction* $ep \to eD^*X'p$ *with* $0.001 < x_{I\!P} < 0.035$. *The inner bars show the statistical uncertainties, and the outer bars correspond to the statistical and systematic uncertainties, added in quadrature. The data are compared to the resolved Pomeron model predictions with the H1FIT2 LO Pomeron parametrization (histogram). The theoretical cross section was normalized to the data. The dashed histogram shows the predicted contribution from resolved photon reactions.*

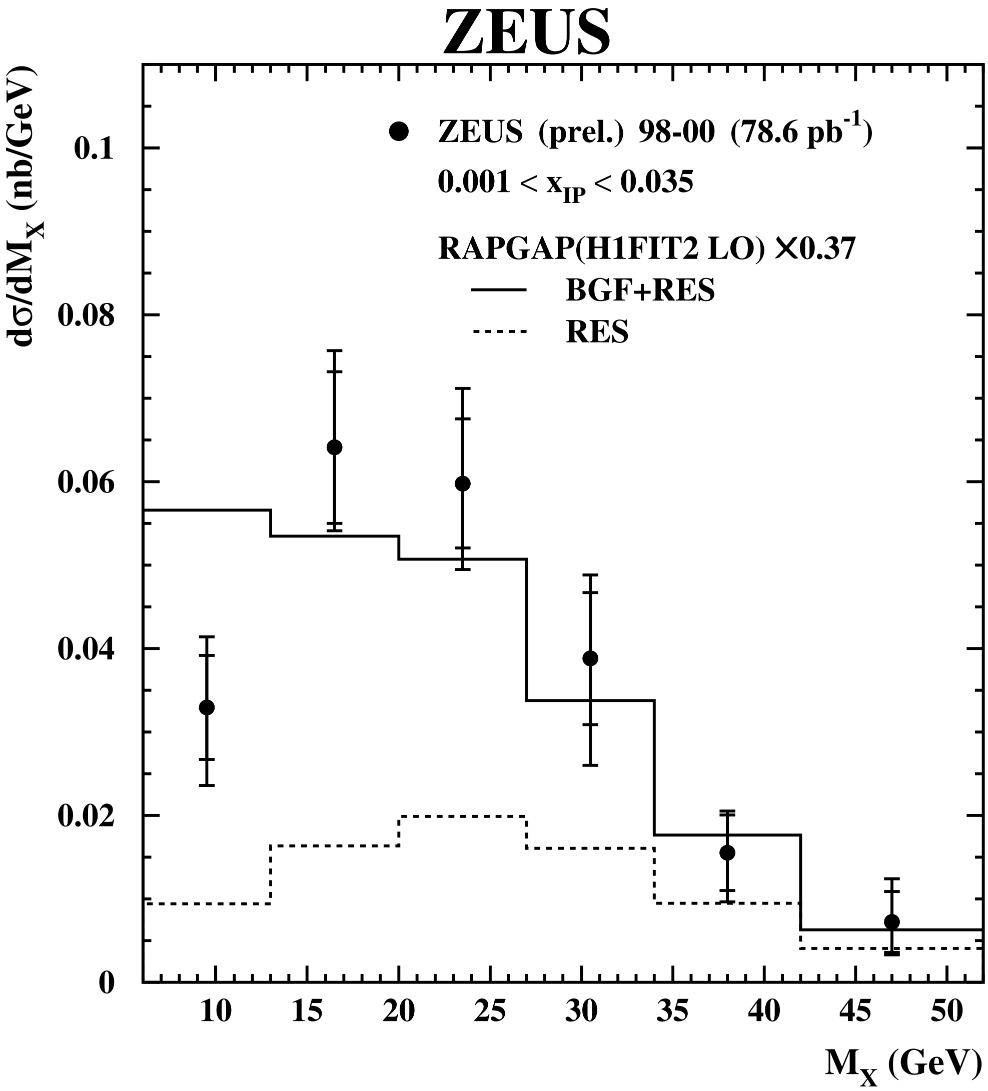

Figure 5: *The cross section $d\sigma/dM_X$ (dots) for the diffractive photoproduction reaction $ep \rightarrow eD^*X'p$ with $0.001 < x_{I\!P} < 0.035$. The inner bars show the statistical uncertainties, and the outer bars correspond to the statistical and systematic uncertainties, added in quadrature. The data are compared to the resolved Pomeron model predictions with the H1FIT2 LO Pomeron parametrization (histogram). The theoretical cross section was normalized to the data. The dashed histogram shows the predicted contribution from resolved photon reactions.*

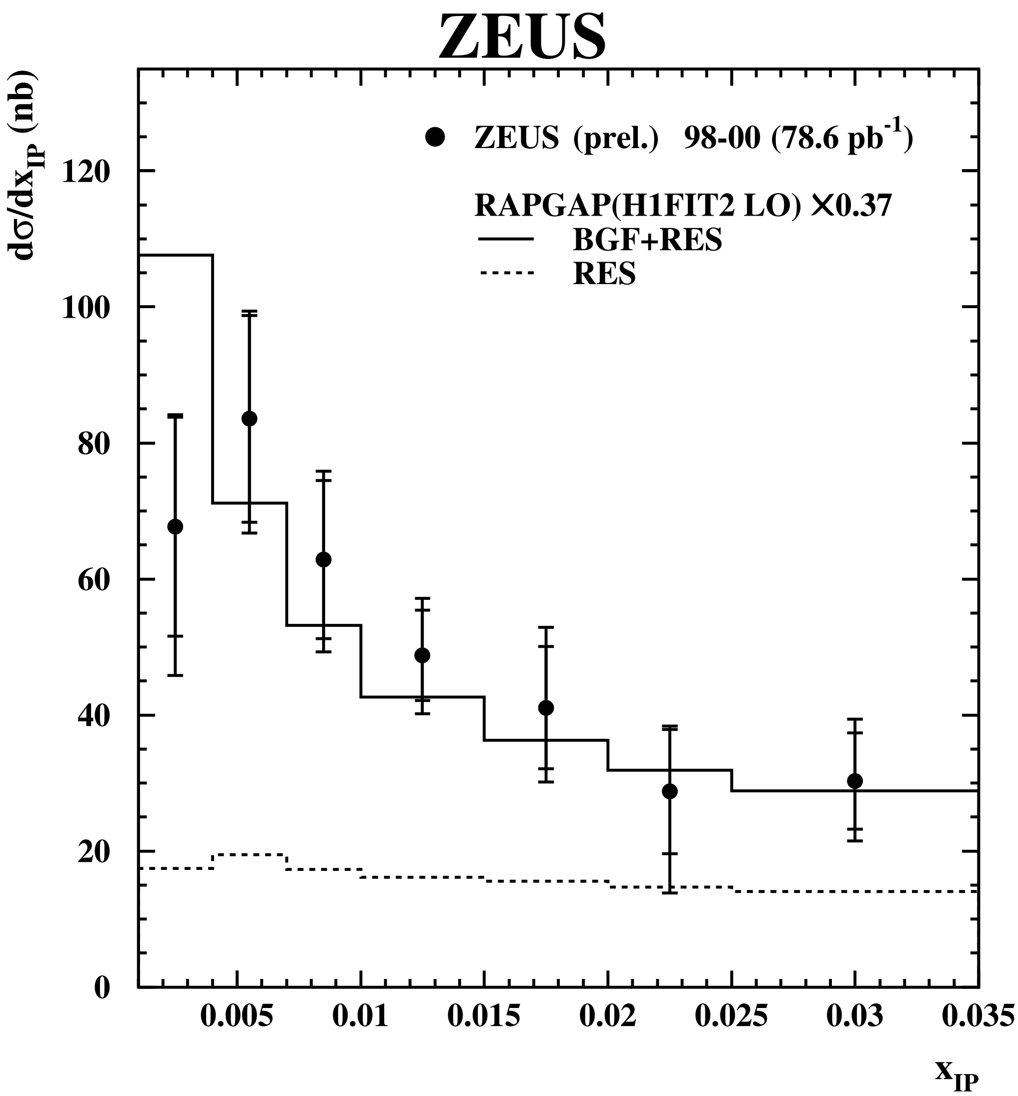

Figure 6: *The cross section $d\sigma/dx_{I\!P}$ (dots) for the diffractive photoproduction reaction $ep \to eD^* X' p$ with $0.001 < x_{I\!P} < 0.035$ The inner bars show the statistical uncertainties, and the outer bars correspond to the statistical and systematic uncertainties, added in quadrature. The data are compared to the resolved Pomeron model predictions with the H1FIT2 LO Pomeron parametrization (histogram). The theoretical cross section was normalized to the data. The dashed histogram shows the predicted contribution from resolved photon reactions.*

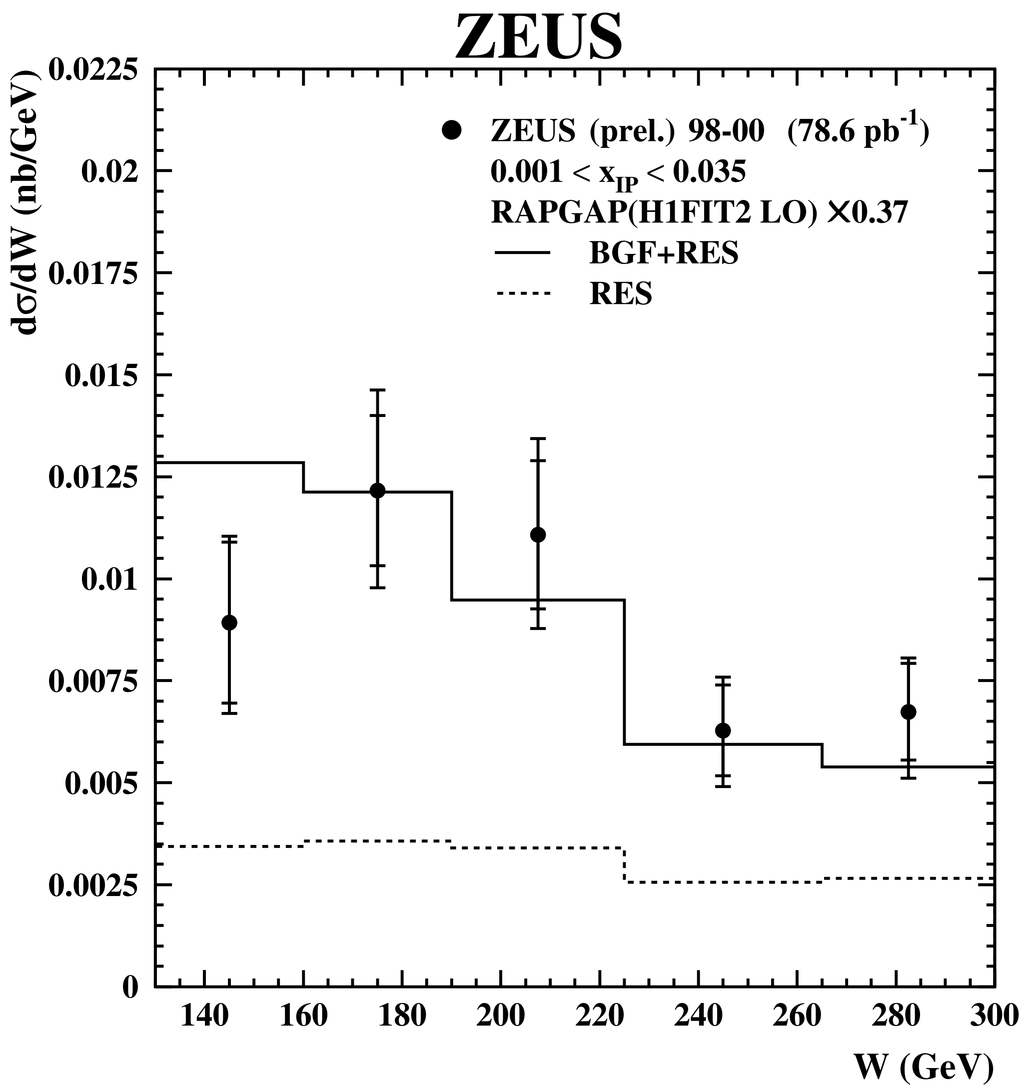

Figure 7: *The cross section $d\sigma/dx_{I\!P}$ (dots) for the diffractive photoproduction reaction $ep \to eD^* X' p$ with $0.001 < x_{I\!P} < 0.35$. The inner bars show the statistical uncertainties, and the outer bars correspond to the statistical and systematic uncertainties, added in quadrature. The data are compared to the resolved Pomeron model predictions with the H1FIT2 LO Pomeron parametrization (histogram). The thoretical cross section was normalized to the data. The dashed histogram shows the predicted contribution from resolved photon reactions.*

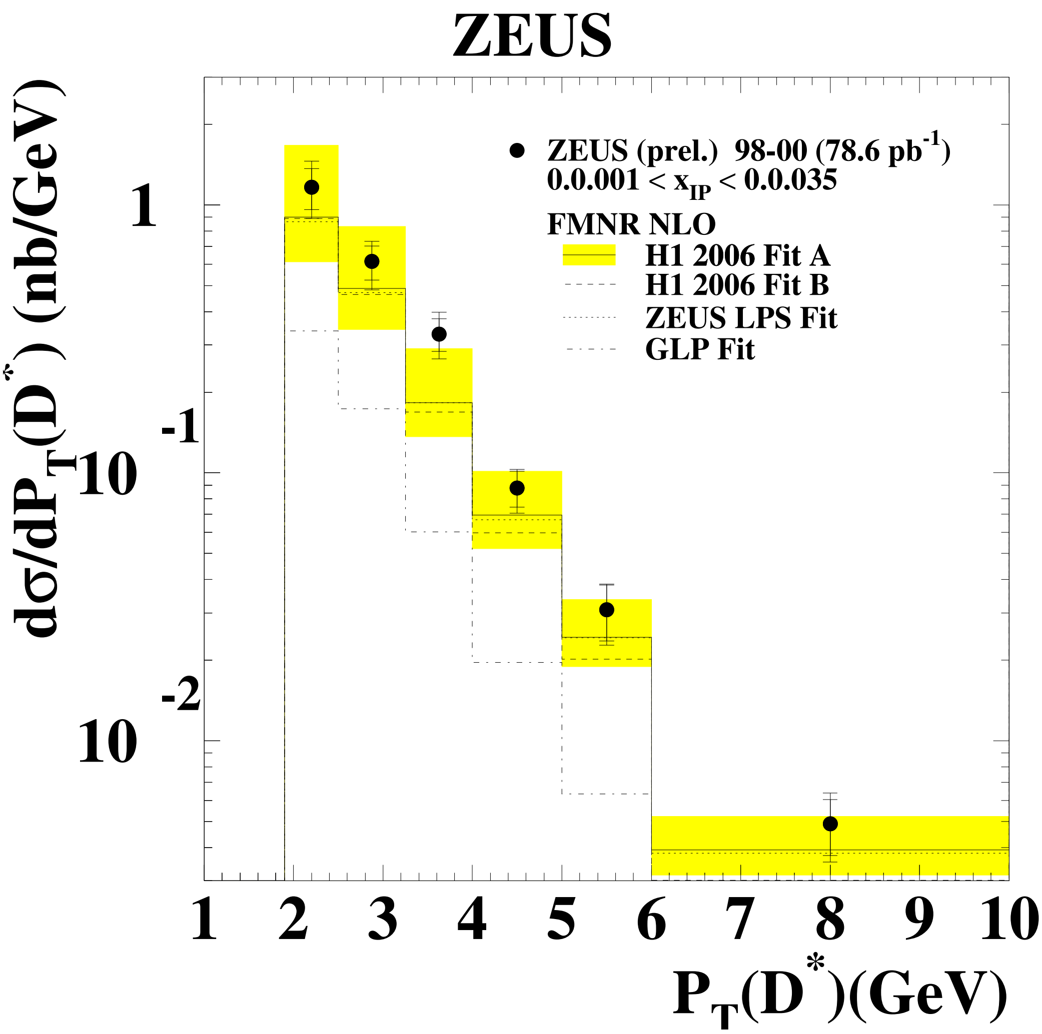

Figure 8: *The cross section $d\sigma/dP_T^{D^*}$ (dots) for the diffractive photoproduction reaction $ep \to eD^*X'p$ with $0.001 < x_{I\!P} < 0.035$. The inner bars show the statistical uncertainties, and the outer bars correspond to the statistical and systematic uncertainties, added in quadrature. The data are compared to FMNR NLO QCD calculations (histograms) with diffractive parton distribution functions, measured from NLO DGLAP QCD fits to the HERA inclusive data on diffraction in DIS. The solid histogram stands for the H1 2006 Fit A, the dashed for the H1 2006 Fit B, the dotted histogram for the ZEUS LPS Fit, and dash-dotted histogram for the GLP Fit. The shaded band shows the uncertainties coming from the charm quark mass and the scale variations.*

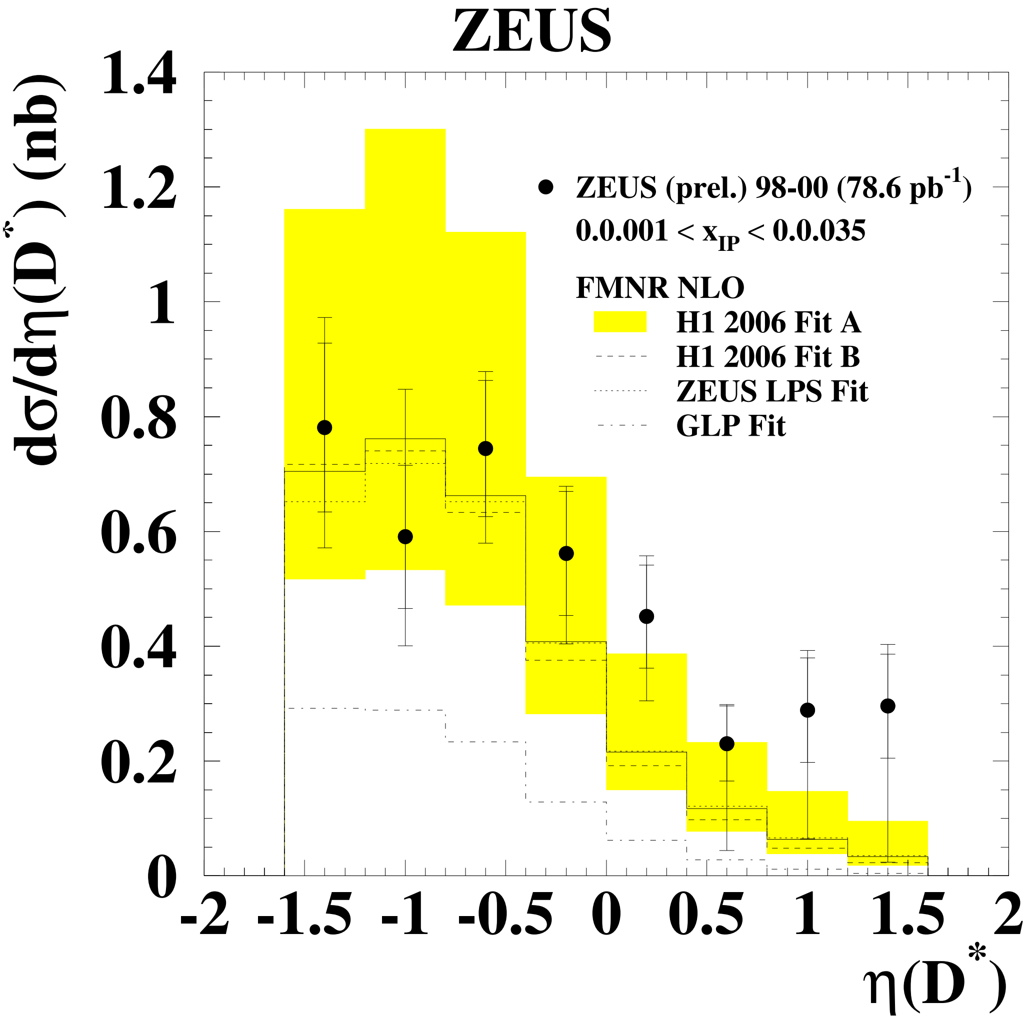

Figure 9: *The cross section $d\sigma/d\eta^{D^*}$ (dots) for the diffractive photoproduction reaction $ep \to eD^*X'p$ with $0.001 < x_{\mathbb{P}} < 0.035$. The inner bars show the statistical uncertainties, and the outer bars correspond to the statistical and systematic uncertainties, added in quadrature. The data are compared to FMNR NLO QCD calculations (histograms) with diffractive parton distribution functions, measured from NLO DGLAP QCD fits to the HERA inclusive data on diffraction in DIS. The solid histogram stands for the H1 2006 Fit A, the dashed for the H1 2006 Fit B, the dotted histogram for the ZEUS LPS Fit, and dash-dotted histogram for the GLP Fit. The shaded band shows the uncertainties coming from the charm quark mass and the scale variations.*

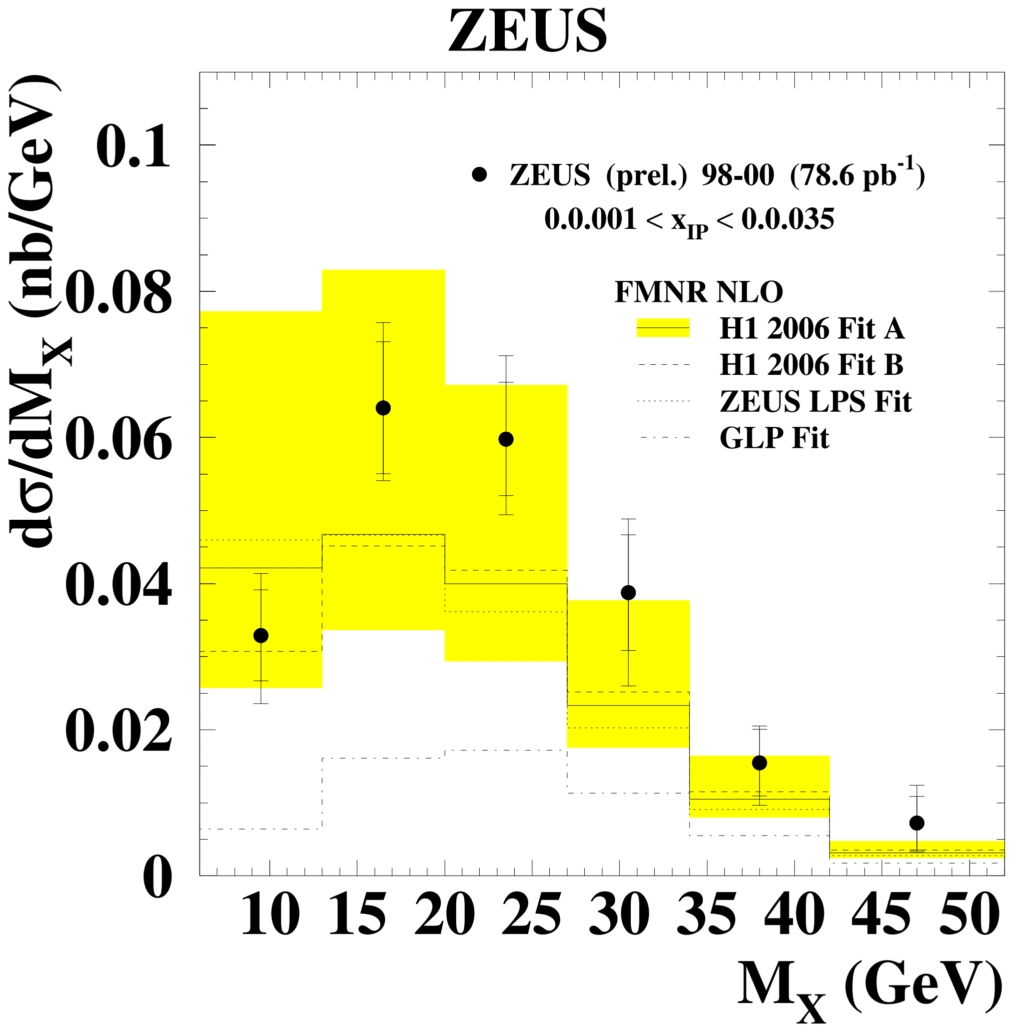

Figure 10: *The cross section* $d\sigma/dM_X$ *(dots) for the diffractive photoproduction reaction* $ep \to eD^* X' p$ *with* $0.001 < x_{I\!P} < 0.035$. *The inner bars show the statistical uncertainties, and the outer bars correspond to the statistical and systematic uncertainties, added in quadrature. The data are compared to FMNR NLO QCD calculations (histograms) with diffractive parton distribution functions, measured from NLO DGLAP QCD fits to the HERA inclusive data on diffraction in DIS. The solid histogram stands for the H1 2006 Fit A, the dashed for the H1 2006 Fit B, the dotted histogram for the ZEUS LPS Fit, and dash-dotted histogram for the GLP Fit. The shaded band shows the uncertainties coming from the charm quark mass and the scale variations.*

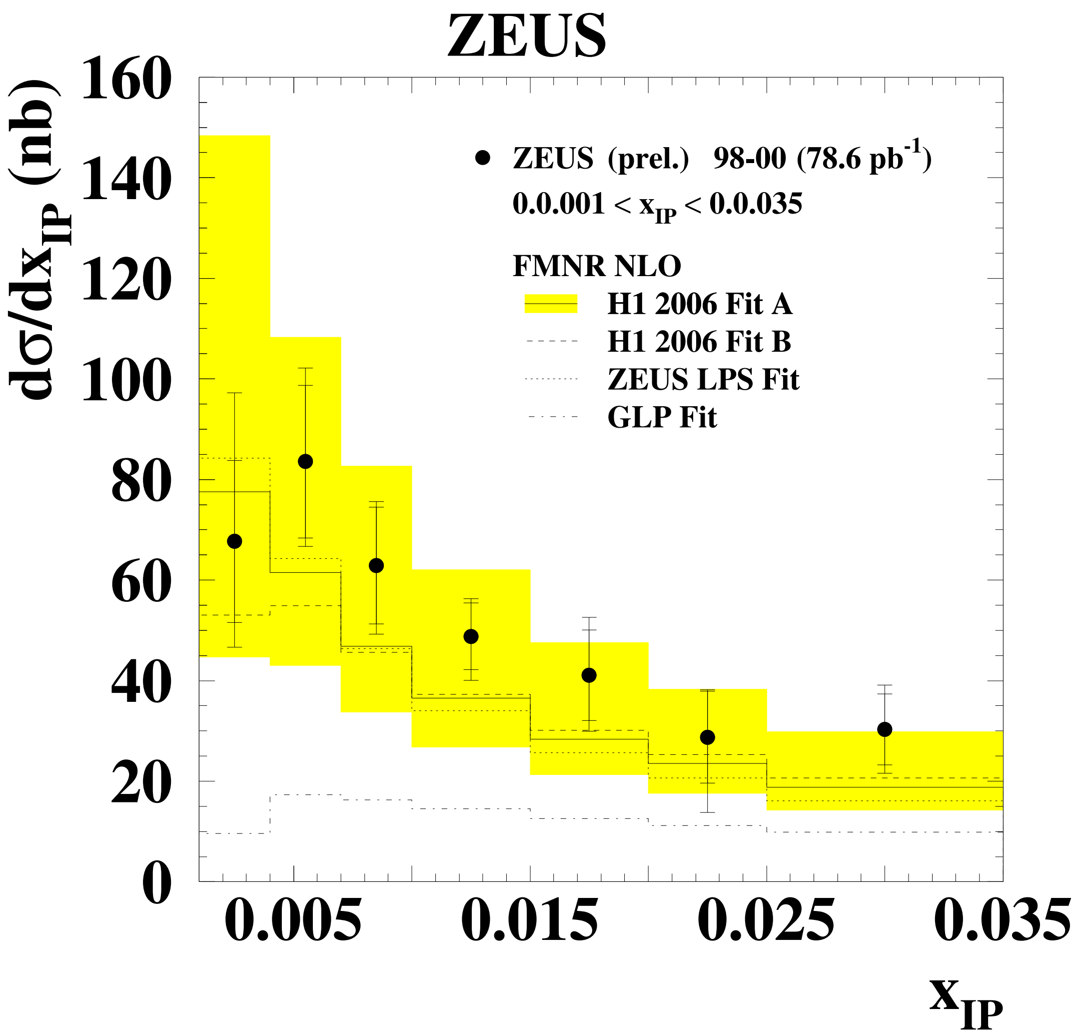

Figure 11: *The cross section $d\sigma/dx_{\mathbb{P}}$ (dots) for the diffractive photoproduction reaction $ep \to eD^*X'p$ with $0.001 < x_{\mathbb{P}} < 0.035$ The inner bars show the statistical uncertainties, and the outer bars correspond to the statistical and systematic uncertainties, added in quadrature. The data are compared to FMNR NLO QCD calculations (histograms) with diffractive parton distribution functions, measured from NLO DGLAP QCD fits to the HERA inclusive data on diffraction in DIS. The solid histogram stands for the H1 2006 Fit A, the dashed for the H1 2006 Fit B, the dotted histogram for the ZEUS LPS Fit, and dash-dotted histogram for the GLP Fit. The shaded band shows the uncertainties coming from the charm quark mass and the scale variations.*

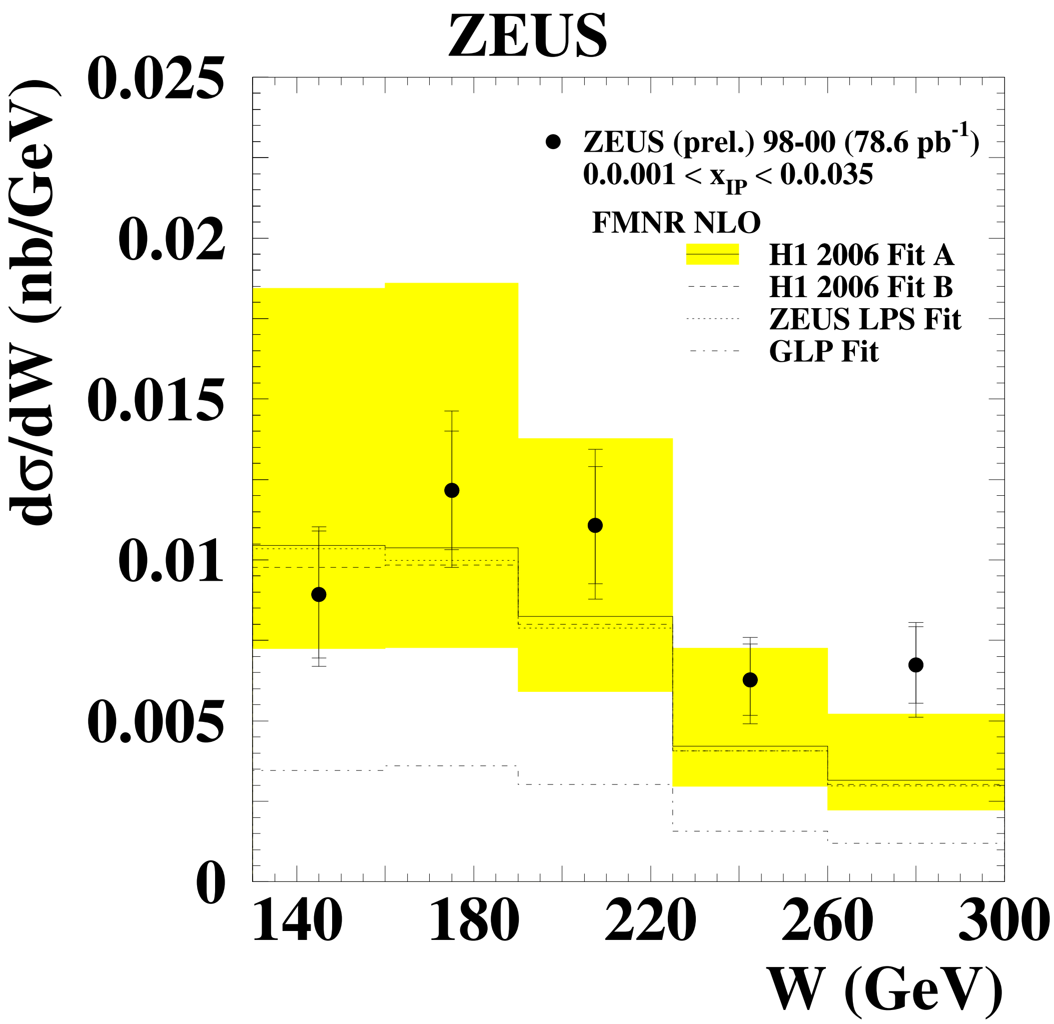

Figure 12: *The cross section* $d\sigma/dW$ *(dots) for the diffractive photoproduction reaction* $ep \rightarrow eD^{*}X'p$ *with* $0.001 < x_{I\!P} < 0.35$. *The inner bars show the statistical uncertainties, and the outer bars correspond to the statistical and systematic uncertainties, added in quadrature. The data are compared to FMNR NLO QCD calculations (histograms) with diffractive parton distribution functions, measured from NLO DGLAP QCD fits to the HERA inclusive data on diffraction in DIS. The solid histogram stands for the H1 2006 Fit A, the dashed for the H1 2006 Fit B, the dotted histogram for the ZEUS LPS Fit, and dash-dotted histogram for the GLP Fit. The shaded band shows the uncertainties coming from the charm quark mass and the scale variations.*